

Peculiar motion of Solar system from the Hubble diagram of supernovae Ia and its implications for cosmology

Ashok K. Singal*

Astronomy and Astrophysics Division, Physical Research Laboratory, Navrangpura, Ahmedabad - 380 009, India

(Dated: June 24, 2021)

Peculiar motion of the solar system, determined from the dipole anisotropy in the Cosmic Microwave Background Radiation (CMBR), has given a velocity 370 km s^{-1} along $\text{RA}= 168^\circ$, $\text{Dec}= -7^\circ$. Subsequent peculiar motion determinations from the number counts, sky brightness or redshift dipoles observed in large samples of distant radio galaxies and quasars yielded peculiar velocities two to ten times larger than CMBR, though in all cases the directions matched with the CMBR dipole. Here we introduce a novel technique for determining the peculiar motion from the magnitude-redshift ($m_B - z$) Hubble diagram of Type Ia Supernovae (SN Ia), one of the best standard candles available. We find a peculiar velocity $1.6 \pm 0.4 \times 10^3 \text{ km s}^{-1}$, about four times larger than the CMBR value, along $\text{RA}= 173^\circ \pm 21^\circ$, $\text{Dec}= 10^\circ \pm 19^\circ$, the direction being within $\sim 1\sigma$ of the CMBR dipole. Since a genuine solar motion would not depend upon the method or the dataset employed, large discrepancies seen among various dipole amplitudes could imply that these dipoles, including the CMBR one, might not pertain to observer's peculiar motion. However, a common direction for various dipoles might indicate a preferred direction in the universe, implying an intrinsic anisotropy, in violation of the cosmological principle, a cornerstone of the modern cosmology.

I. INTRODUCTION

Exploiting SNe Ia as standard candles, cosmological parameters have been derived, which suggested a Universe with accelerating expansion rate [1–5]. Some reservations have recently been expressed on these results [6, 7], but these have been refuted elsewhere [8, 9]. One important element in these studies is the estimate of the local bulk flow [10]. For instance, no clinching evidence for such bulk flow from type Ia supernovae has been found [11]. On the other hand, bulk flows $v_{\text{bf}} \sim 170$ to 540 km s^{-1} in the nearby universe ($z \lesssim 0.06$) have also been reported [12–15]. In all these studies, the observed heliocentric redshifts and magnitudes of SNe were corrected for the peculiar velocity of the observer, derived from the CMBR dipole to be 370 km s^{-1} in the direction $\text{RA}= 168^\circ$, $\text{Dec}= -7^\circ$ [16–18]. However, an unexpected, substantially bigger dipole anisotropy, observed in a large sample of distant radio sources, yielded a peculiar motion ~ 4 times [19] the CMBR value, though in the same direction as the CMBR dipole. Subsequent confirmations of the peculiar velocity with respect to AGN reference frames being much larger than the CMBR value [20–28], cast doubts on the CMBR dipole being the ultimate representatives of the solar peculiar motion. It might be desirable to determine the peculiar velocity with respect to a different reference frame, and if possible using an independent method, to examine whether the derived peculiar motion is indeed significantly larger than that inferred from the CMBR dipole. Here we introduce such a novel technique and apply it to determine peculiar motion of the observer, from the magnitude-redshift Hubble diagram for the SNe Ia, one of the best standard candles known.

II. PECULIAR MOTION FROM THE HUBBLE DIAGRAM

Due to a peculiar velocity v of the observer, the observed redshift and optical magnitude of an object, lying at an angle θ with respect to the direction (pole) of the peculiar motion, will get modified as [29]

$$(1+z) = (1+z_o)(1-v \cos \theta/c), \quad (1)$$

$$m = m_o + 5 \log(1-v \cos \theta/c), \quad (2)$$

where z_o , m_o are the values as would be measured by a comoving observer, i.e., without any peculiar motion. Here v is assumed to be non-relativistic ($v \ll c$) since all previous dipole measurements have indicated so.

For a given peculiar velocity v of the observer, different sources, depending upon their angle θ , will get differently displaced, according to Eqs. (1) and (2), in the Hubble $m - z$ plot. As the effects on both m and z are proportional to $\cos \theta$, all source with $\cos \theta > 0$, and thus lying in a hemisphere, say Σ_1 , centred on the pole of peculiar motion, will get displaced in the $m - z$ plot opposite to the sources with $\cos \theta < 0$ and thus lying in the opposite hemisphere, say Σ_2 , centred on the anti-pole. Accordingly, in the Hubble diagram, there will be a systematic shift between sources belonging to the two hemispheres, Σ_1 and Σ_2 . This systematic shift provides a measure of the peculiar velocity of the observer, or equivalently that of the solar system.

Here we apply this novel technique to successfully determine the peculiar motion of the solar system, from the magnitude-redshift Hubble diagram for SNe Ia, which are one of the best standard candles known, with a very tight $m_B - z$ relation, where m_B denotes the observed peak blue magnitude and z the measured redshift of each SN Ia. As we shall see, this technique, unlike other methods employed to estimate our peculiar motion, e.g. number counts or sky brightness from AGN surveys compris-

* ashokkumar.singal@gmail.com

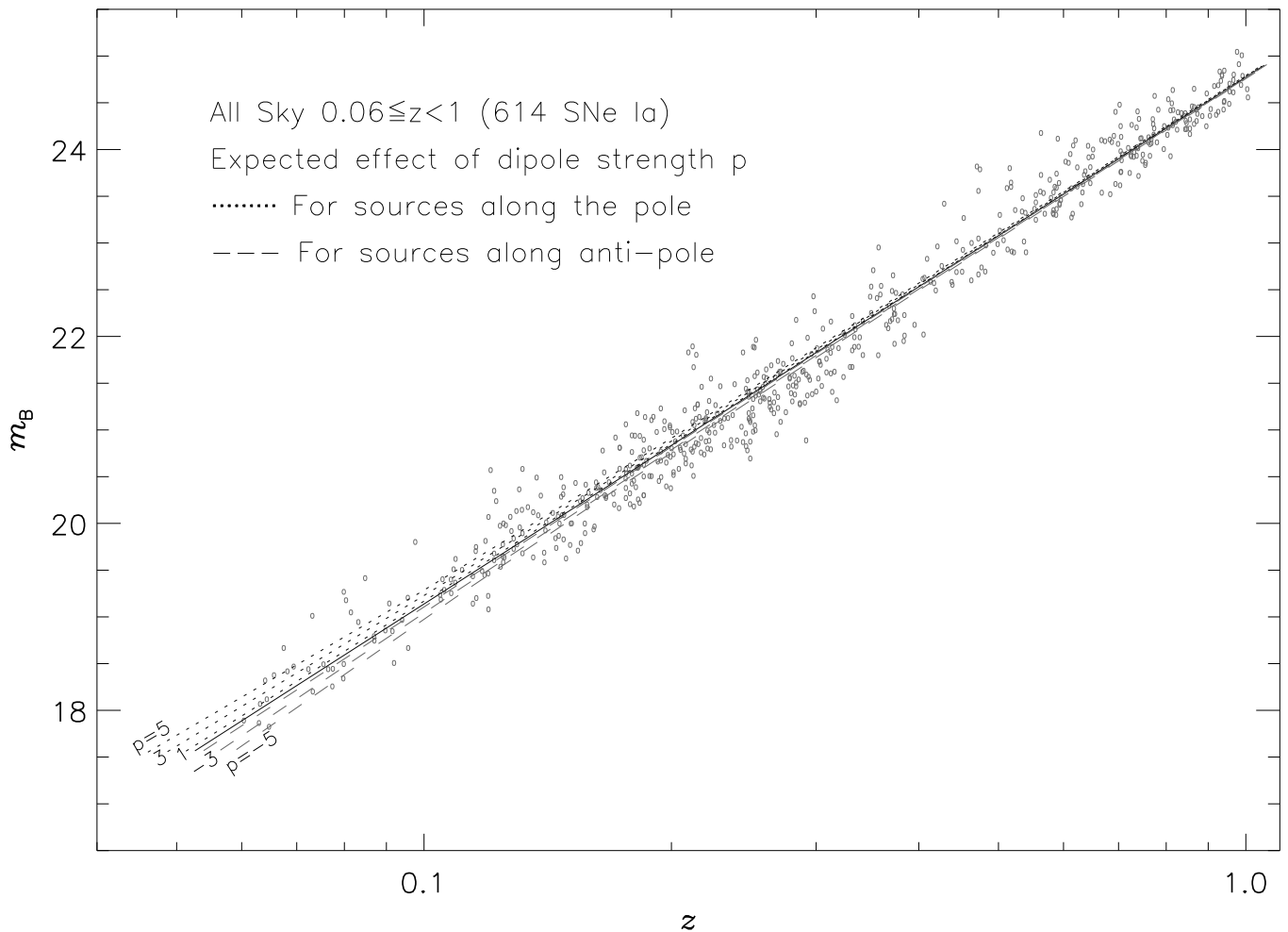


FIG. 1. The observed Magnitude-redshift ($m_B - z$) distribution of SNe Ia in our sample. The dark continuous line in the middle shows the straight line fit with $m_B \propto \log z$, to all SNe Ia in our sample. Due to observer’s peculiar velocity, assumedly along the CMBR dipole, individual sources at any point in the $m_B - z$ diagram would get displaced, with the displacement being, to a first order, directly proportional to the amplitude of the peculiar velocity, assumed to be a small non-relativistic value. The family of gray dotted lines at higher m_B above the continuous line show the displacements expected for different amplitudes of the peculiar velocity (quantified by p , in units of the CMBR value of 370 km s^{-1}), the loci of the expected displacements for sources lying in the direction (pole) of the peculiar velocity at its apex, while the dashed lines below the continuous line show loci of the displacements expected for sources lying in the anti-pole direction, for different p values ($p < 0$ in the anti-pole direction).

ing $\gtrsim 10^5$ sources [19–28], can yield statistically significant results from much smaller number ($\lesssim 10^3$) of SNe. Moreover, the completeness of the survey, an absolute requirement in other methods where all sources above a certain observed flux density limit are part of the sample, is not a prerequisite. Nor is the full sky-coverage essential; a piece-wise coverage of the sky in different directions could suffice. In fact, it could as such be applied to a combination of data from a heterogeneous set of various sub-samples; all that is required is that no systematic errors have observationally entered in the redshift and magnitude estimates of individual sources lying in different directions in sky.

III. OUR SAMPLE OF SNE IA AND THE PROCEDURE DEPLOYED FOR COMPUTING THE PECULIAR MOTION

For our purpose, we have selected a restricted sub-sample of the JLA sample [3] which contained 740 spectroscopically confirmed SNe Ia, spanning a redshift range 0.01-1.3. However, we have restricted for our purpose the lower limit to 0.06 in order to keep the effect of local bulk flows to a minimum [7]. Further, there are only 8 SNe Ia in the JLA sample with $z > 1$, which we have excluded leaving us with a total of 614 SNe Ia in our sample. The ‘corrections’ already applied for the peculiar velocity of the solar system, as derived from the CMBR dipole, to the redshift and magnitude values have been reverted to

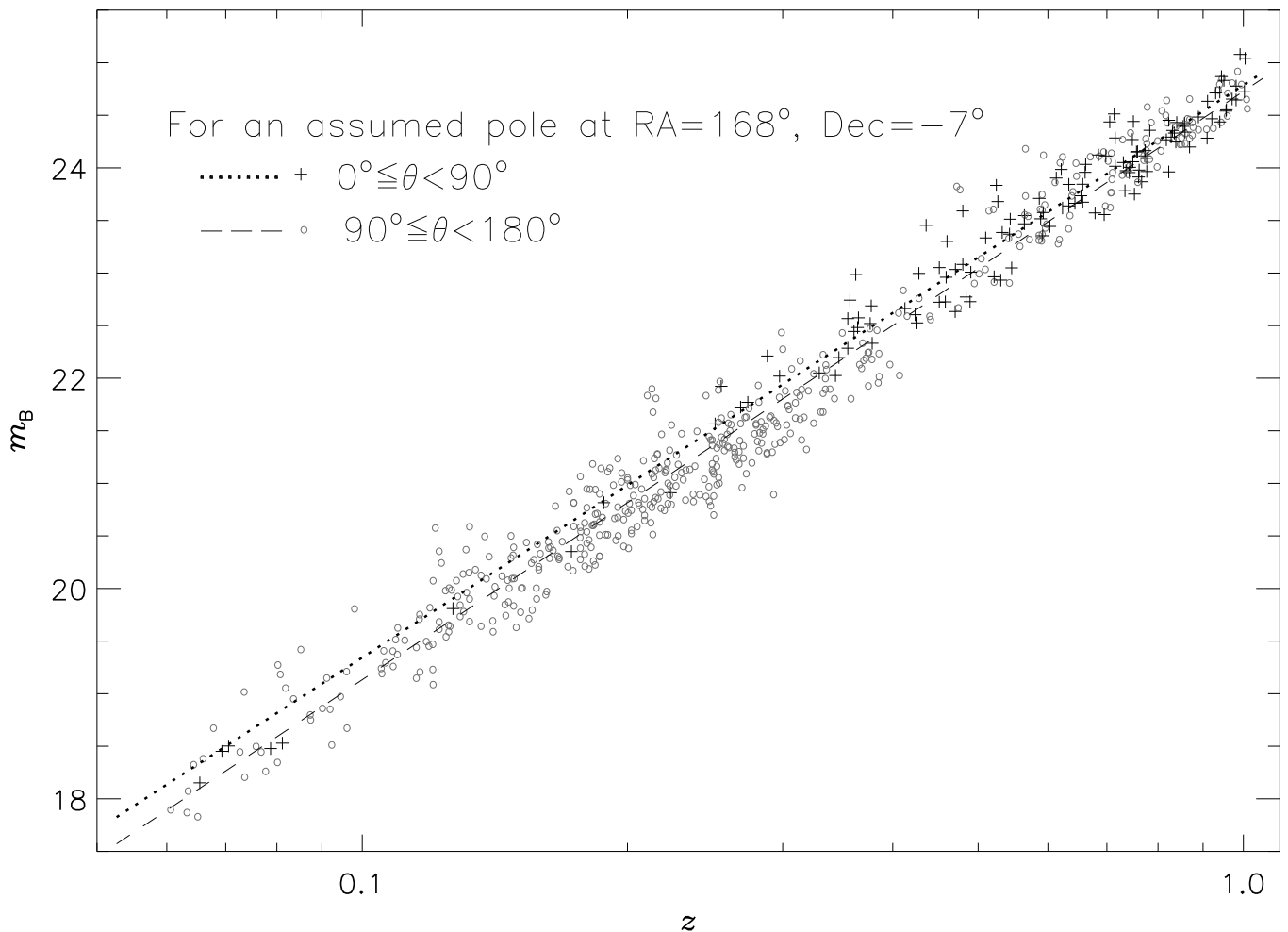


FIG. 2. The observed Magnitude-redshift ($m_B - z$) distribution of SNe Ia in the sky. The dotted line shows the straight line fit to SNe Ia, denoted by plus (+) symbols, in the Σ_1 hemisphere centred on the CMBR pole, while the dashed line shows the straight line fit to SNe Ia, denoted by circles (o), in the Σ_2 hemisphere, centred on the CMBR anti-pole. The two lines show from each other, especially at low redshifts, say at $z \sim 0.06$, a displacement Δm_B which, to a first order, is proportional to (the component of) the observer's peculiar velocity in the CMBR dipole direction, and thus is a measure of $p \cos \psi$, with ψ being the angle of the CMBR dipole from the true dipole direction.

get back the observed heliocentric values.

Figure 1 shows the peak blue magnitude versus redshift ($m_B - z$) Hubble plot, made for our sample of SNe Ia, covering the whole sky. If there were no peculiar motion of the observer, then the observed ($m_B - z$) relation could be employed directly to test various cosmological models. However due to a peculiar motion of the observer, there could be alterations in the $m_B - z$ plot. We can use a parameter p to express the amplitude of the peculiar velocity v , in units of the CMBR value, so that $v = p \times 370 \text{ km s}^{-1}$, with $p = 0$ implying a nil peculiar velocity while $p = 1$ implying the CMBR value.

Let us first assume that the peculiar velocity is along the CMBR dipole, $\text{RA} = 168^\circ$, $\text{Dec} = -7^\circ$. Then using the great circle at 90° from this pole direction, we divide the sky in two equal hemispheres, Σ_1 and Σ_2 , with Σ_1 containing the above pole, and Σ_2 containing the anti-

pole. Individual sources at any point in the $m_B - z$ diagram would get displaced, with the displacement being, to a first order, directly proportional to the amplitude of the peculiar velocity, assumed to be a small non-relativistic value. In Fig. 1, the dark continuous line, which is a straight line fit to the observed $m_B \propto \log z$ data, can be taken to be for $p = 0$, since there may be an overlap of sources distributed evenly in both Σ_1 and Σ_2 hemispheres. The set of grey dotted lines above (at m_B values higher than) the $p = 0$ line show, for an increasing p , the loci of expected displacements for sources lying in the hemisphere Σ_1 , while the grey broken lines below the continuous line show loci of the displacements expected for sources in Σ_2 ($p < 0$ in this direction). Thus a difference in magnitude Δm_B between sources lying in Σ_1 and Σ_2 at some given low enough redshift, say $z = 0.06$, yields value of p for the peculiar motion. It should be

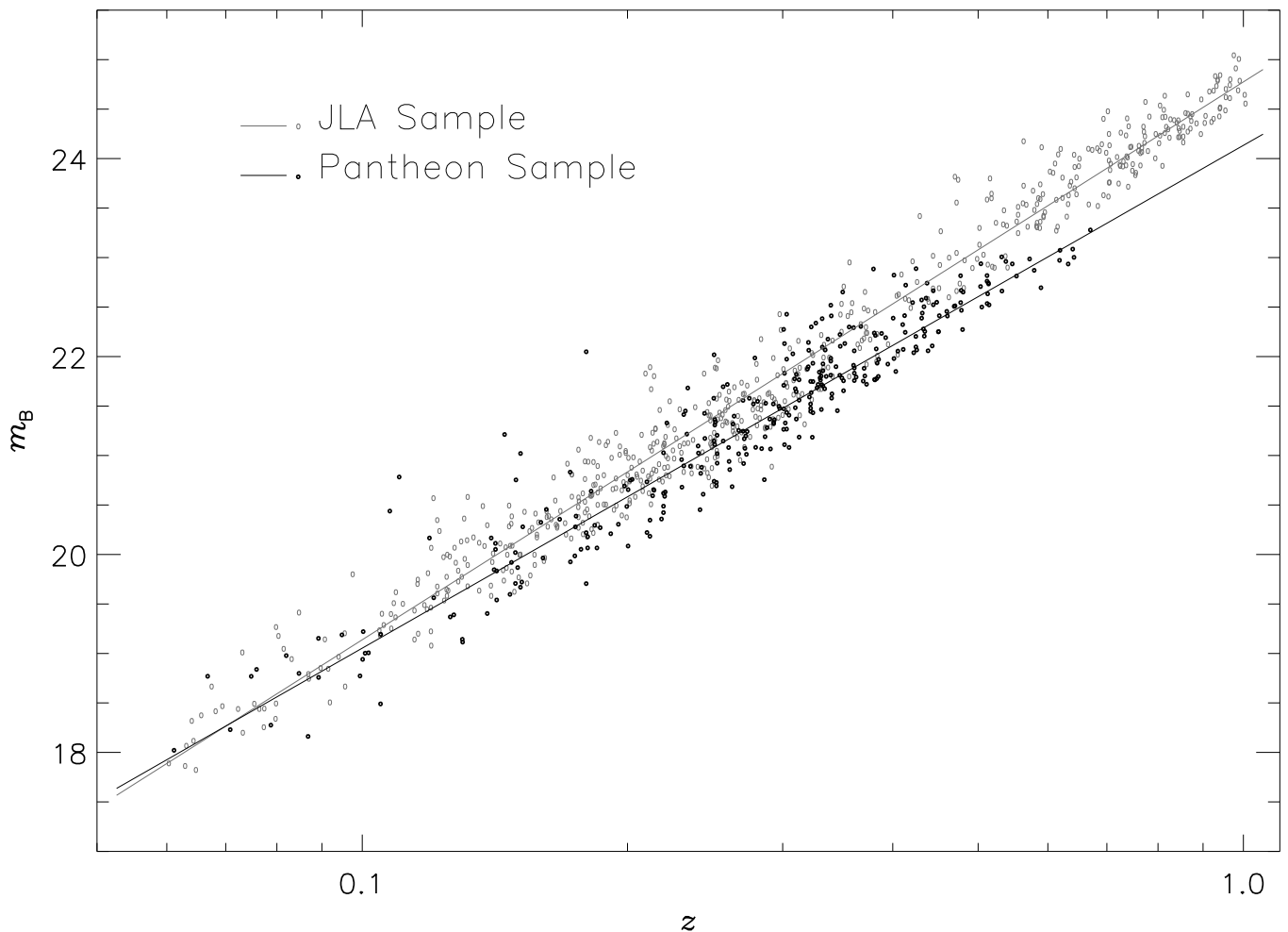


FIG. 3. A comparison of the Magnitude-redshift ($m_B - z$) distribution of SNe Ia in the JLA (fainter gray points) and Pantheon samples (darker points). Although the two samples seem to match at low redshifts ($z \sim 0.06$), at higher redshifts they progressively depart in magnitude (m_B), so much that at $z \sim 0.6$, the Pantheon sample is systematically brighter than the JLA sample by $\Delta m_B \approx -0.5$.

noted that in Fig. 1, plots depicted for various p values are for sources along the pole or anti-pole direction. For an even distribution of sources along various directions within each hemisphere, the net displacement will on the average be half of that shown in Fig. 1 for each p value.

Figure 2 shows the actual displacement that occurs in the $m_B - z$ diagram between sources in two opposite hemispheres, taking the peculiar motion to be along the CMBR dipole. The dotted line above and the dashed line below depict a fit to the actual $m_B - z$ plots for sources, separately in the Σ_1 and Σ_2 hemispheres. From a comparison with the loci in Fig. 1 of the expected displacements for sources lying in the two hemispheres, the observed displacement between the dotted and dashed lines in Fig. 2 suggests $p \gtrsim 4$, instead of $p = 1$, expected for the CMBR dipole. The inferred p value, at least to a first order, will be proportional to $\cos \psi$, the projection of the assumed dipole, CMBR here, on the actual dipole, if the latter is along a different direction. It is

evident that the peculiar velocity is certainly not concordant with the CMBR value, which should have given $p \approx 1$. At higher redshifts, not only are the displacements relatively smaller in amplitude they are also almost along the $p = 0$ line, while at lower redshifts the amplitudes of displacement seem much larger and are off the $p = 0$ line (Fig. 1). A higher degree polynomial fit than a straight line may not be essential for our purpose, as the displacements in the $m_B - z$ plot, as evident from Fig. 1, are predominantly at lower redshifts, where differences between various cosmological models are not significant.

In our sample there are only 128 SNe in the hemisphere Σ_1 while 486 SNe belong to Σ_2 , in fact, there is a particular deficiency in Σ_1 of sources in the z range 0.08 to 0.3. This comes from the sky coverage in various subsamples of the JLA sample. A somewhat even split of sources amongst Σ_1 and Σ_2 would minimize statistical uncertainties in the mutual displacement estimates. In order to have additional sources in the Σ_1 hemisphere,

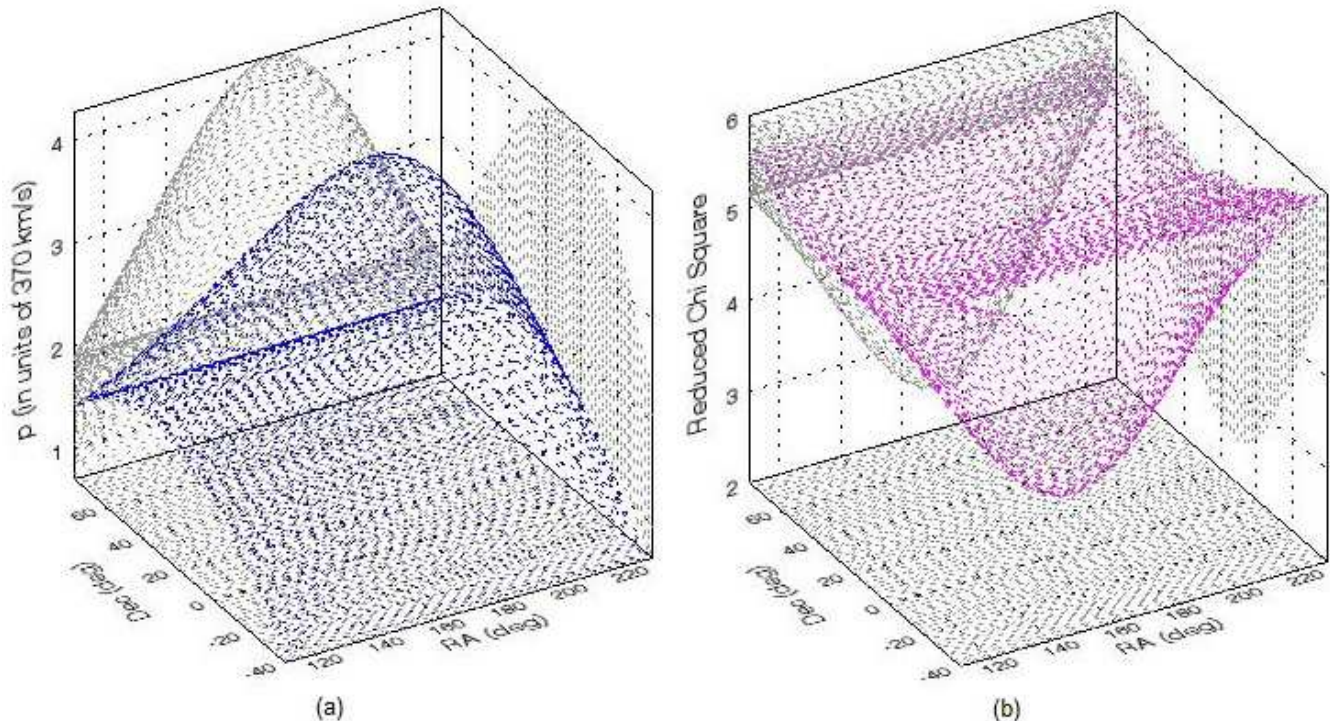


FIG. 4. A plot of 3-d cos fits made to the estimated p values for various trial dipole directions across the sky, showing (a) a unique peak (blue colour) along RA= 175°, and Dec= 8°, which unambiguously indicates the optimum direction of the dipole (b) reduced chi-square (χ^2_{ν}) (violet colour), having a minimum value of 2.5 (somewhat higher than the ideal value of unity) at RA= 171°, and Dec= 12°. The horizontal axes denote RA and Dec in degrees. The positions (RA and Dec) of the extrema are determined more easily from the 2-d projections, shown in light grey. Thence we infer the direction of the observer’s peculiar velocity as RA= 173°, and Dec= 10°, within $\sim 1\sigma$ of the CMBR dipole direction, however the amplitude appears to be a factor ~ 4 higher than the CMBR value.

we examined the Pantheon sample of 300 plus SNe [4, 5] for inclusion in our study. However, it has been reported that the Pantheon sample may have significant discrepancy in redshift values as compared to the JLA sample data [30]. To investigate suitability of the Pantheon samples for our purpose, we made the $m_B - z$ plot of SNe Ia belonging to both JLA and Pantheon samples separately in the same diagram. Figure 3 shows the $m_B - z$ plots and straight line fits for both samples. In order to distinguish the two plots, we have used light gray points for the JLA data and also shown the straight line fit to the $m_B - \log z$ plot by a light colour line as compared to that for the fit to the Pantheon data. It is clear that there is a systematic difference in the two data. Although the two samples seem to match at low redshifts ($z \sim 0.06$), at higher redshifts they progressively depart in magnitude (m_B), so much that at $z \sim 0.6$, the Pantheon sample is systematically brighter than the JLA sample by $\Delta m_B \approx -0.5$. It should be noted that the data in both cases has been reduced to the Heliocentric system by reverting any corrections that had been made to m_B as well as z for the assumed peculiar motion with respect to the CMBR. For the present purpose we shall confine ourselves to the JLA sample alone.

In Fig. 2, we had assumed the peculiar motion to be along the CMBR dipole, however, the actual direction of the peculiar motion might be different. To get a handle on the true direction of the SNe Ia dipole, without a bias toward any particular direction, including that toward the CMBR dipole, we used ‘the brute force method’ [25] by dividing the sky into pixels of $2^\circ \times 2^\circ$, creating a grid of 10360 cells covering the whole sky area of 4π sr (= 41253 square degrees), with minimal overlaps. Then taking the trial pole direction to be the centre of each of these 10360 pixels, we compute one by one the dipole amplitudes (p), along with standard errors, from the best fits to the $m_B - z$ data for all our 614 SNe Ia. This actually yields only a projection of the actual peculiar velocity along each chosen pole direction. Therefore, we can expect a peak along the real dipole direction, along with a $\cos \psi$ dependence in the p values, determined for various grid points around it. Although a broad plateau showing maxima in p , towards certain band of directions was discernible, due to fluctuations in individual values it was not possible to zero down on a single unique peak for the true dipole direction. However, because of the expected $\cos \psi$ dependence of p for grid points around, for each of the $n = 10360$ positions we made a 3-d cos fit to

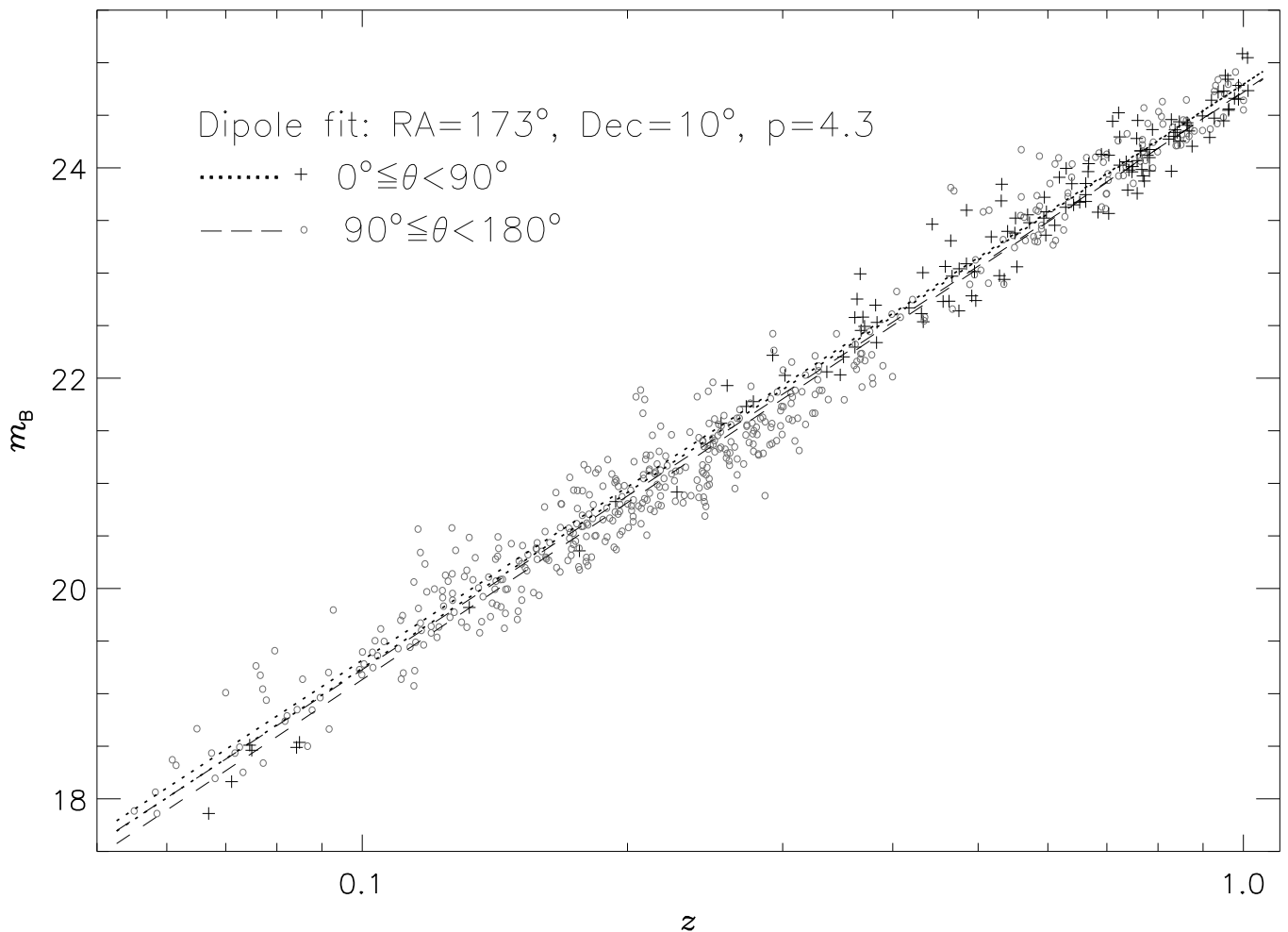


FIG. 5. The observer’s peculiar velocity from the $m_B - z$ plot of SNe Ia is given by a dipole along $RA=173^\circ$, $Dec=10^\circ$ with $p = 4.3$. The upper dotted line represents the fit to the heliocentric SNe Ia data in Σ_1 hemisphere, while the lower dashed line represents the same for the Σ_2 hemisphere. Both data, shown as plus (+) and circle (o) symbols in the plot, after correcting for the peculiar velocity $v = 4.3 \times 370 \text{ km s}^{-1}$ are when fitted separately, the dotted and dashed lines almost coincide in the middle.

the remaining $n - 1$ p values around it, and determined the optimum dipole from the peak values as well as the minimum χ^2 for these n fits.

The process converged reasonably well to show an unambiguous peak for the optimum dipole at $RA=175^\circ$, $Dec=8^\circ$ (Fig. 4a), along with the reduced χ^2 showing a unique minimum in the close vicinity at $RA=171^\circ$, $Dec=12^\circ$ (Fig. 4b). A grid size of $1^\circ \times 1^\circ$, with more than 41000 cells, or a still finer grid size of $0.5^\circ \times 0.5^\circ$ made no perceptible difference in our results.

To validate our cos fit procedure, we made Monte Carlo simulations, by allotting random positions (RA and Dec) in the sky to SNe in our sample and then a mock dipole was superimposed to calculate z and m_B for each source according to Eqs. (1) and (2). Then for this mock catalogue of SNe Ia, our procedure was applied to recover the dipole and compared with the input mock dipole in that simulation. This not only tested our method but it also

provided us an estimate of errors from 2500 independent Monte Carlo simulations, made in five sets of 500 each, so as to be sure that results from simulations, including the error estimates, are consistent across different sets of 500 simulations.

IV. RESULTS AND CONCLUSIONS

Following a simple kinematic approach, without ascribing to any particular cosmological model, we have attempted to extract out the purely special relativistic or even non-relativistic Doppler effects of the observer’s (Solar system’s) peculiar motion, by making an appropriate (first degree) polynomial fit to the Hubble plot. From that we obtain our peculiar velocity to be along $RA=173^\circ \pm 21^\circ$, $Dec=10^\circ \pm 19^\circ$, with $p = 4.3 \pm 1.1$, a 3.9σ result. In fig. 5 are shown the dotted and dashed

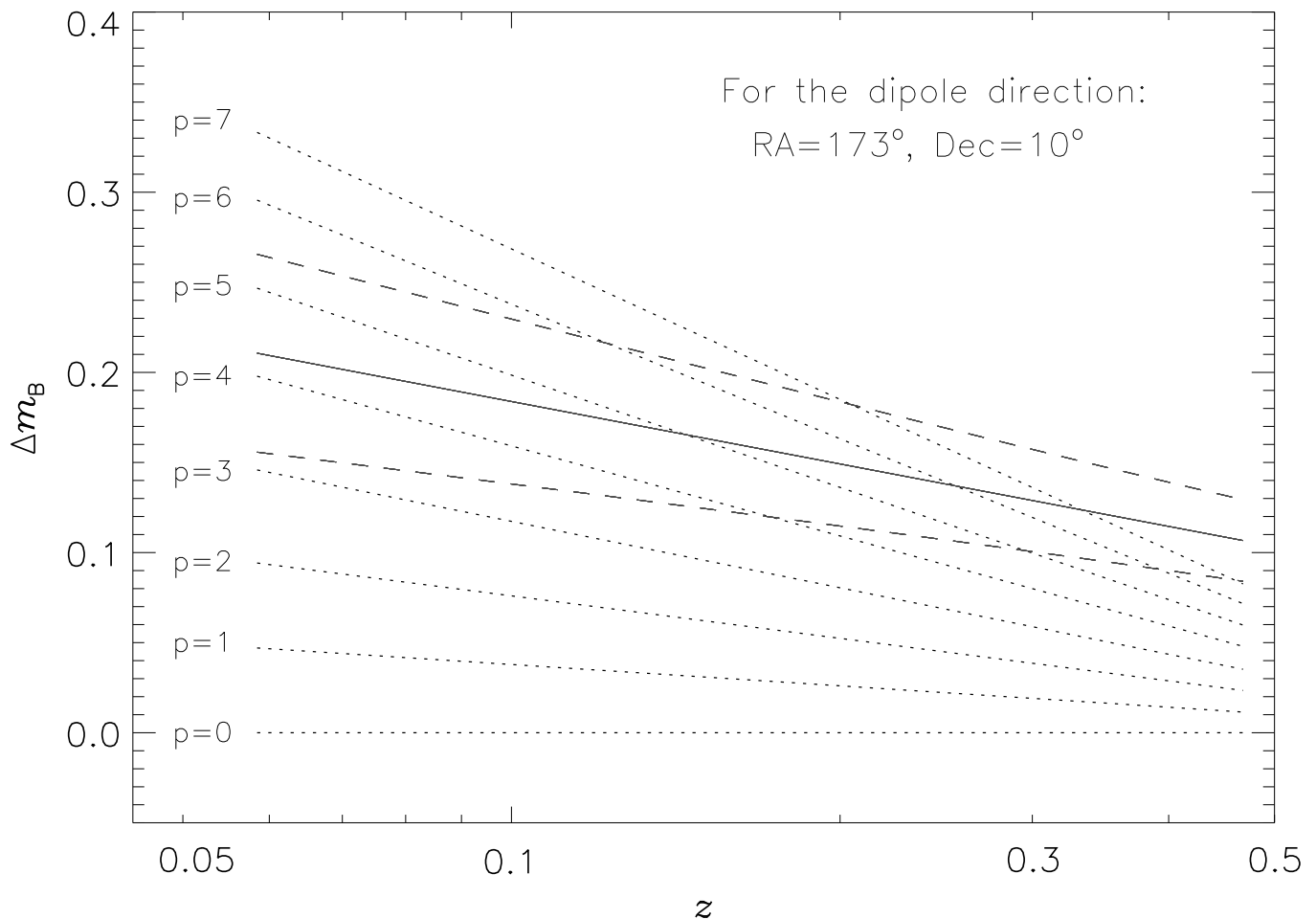


FIG. 6. For observer’s peculiar velocity direction along $RA=173^\circ$, $Dec=10^\circ$, the expected differences Δm_z between average magnitudes of sources from the two hemispheres, Σ_1 and Σ_2 , plotted as dotted lines, for different peculiar velocity values ($p = 0$ to 7). The unbroken line shows a fit to the actual observed difference at different redshifts in the average magnitudes of sources from the two hemispheres, while the dashed lines above and below the unbroken line represent the 1σ uncertainties in the fit.

lines, fits to sources in Σ_1 and Σ_2 hemispheres respectively, which after the corrections for the above dipole is applied, almost coincide, especially at lower redshifts, where a large mutual displacement had otherwise appeared between sources belonging to Σ_1 and Σ_2 , because of observer’s peculiar velocity. To demonstrate it more explicitly, in Fig. 6 we have plotted the expected differences Δm_z between average magnitudes of sources from the two hemispheres, Σ_1 and Σ_2 , plotted as dotted lines, for different peculiar velocity values ($p = 0$ to 7) of the observer along $RA=173^\circ$, $Dec=10^\circ$. The unbroken line shows a fit to the actual observed difference at different redshifts in the average magnitudes of sources from the two hemispheres, again for the peculiar velocity direction along $RA=173^\circ$, $Dec=10^\circ$, while the dashed lines above and below the unbroken line represent the 1σ uncertainties in the fit.

Though the uncertainty in the pole position for the SNe Ia dipole direction is large, but it agrees, within $\sim 1\sigma$, with the CMBR dipole direction, $RA=168^\circ$, $Dec=$

-7° . However the amplitude of the velocity, $1.6 \pm 0.4 \times 10^3$ km s^{-1} , is $\gtrsim 4$ times the CMBR value, our derived motion though seems to be in excellent agreement with the value [19–22] derived from the NRAO VLA Sky Survey [31] data as well as that derived recently [27, 28] from the number counts of mid infra red AGNs [32], but is smaller than [23, 24] that derived from the TIFR GMRT Sky Survey data [33, 34] or the DR12Q data [25] from the Sloan Digital Sky Survey III [35].

In order to ascertain that there are no effects of some skew distribution in our sample, we divided our JLA sample into two equal halves by picking the odd numbered or even numbered sources in our list and then applying the above procedures separately for each of the two sub-samples. We got almost the same results in each of these two sub-samples. The values we obtained for the peculiar velocity for the two sub-samples respectively were $p = 5.1 \pm 1.7$ along $RA=182^\circ \pm 29^\circ$, $Dec=15^\circ \pm 23^\circ$, and $p = 3.6 \pm 1.4$ along $RA=157^\circ \pm 33^\circ$, $Dec=11^\circ \pm 26^\circ$. The difference in the pole positions and p values are well

within the quoted statistical uncertainties.

A factor of $\gtrsim 4$ in the peculiar velocity derived here from SNe Ia as compared to the CMBR value, as well as the earlier derived large factors of two to ten in the dipole amplitudes from various AGN datasets [19–28] may perhaps be pointers to the need for some rethinking on the conventional interpretation of these dipoles, especially, whether these dipoles do pertain to the peculiar motion of the Solar system. At the same time, an alignment of dipole directions in all cases cannot be fortuitous and is perhaps an indication of a preferred direction in the cosmos, which would imply a breakdown of the cosmological principle, the basic foundation over which the edifice of the modern cosmology has been erected.

The cosmological parameters from SNe Ia data have been determined in the literature [1–9] using a peculiar velocity of the observer, as derived from the CMBR dipole, to reduce the heliocentric redshifts to the comoving reference frame. However, a larger peculiar motion would necessitate a fresh look at these determinations, more so as the fits to the $m_B - z$ plots vis-à-vis theoretical curves of various cosmological models get anchored at lower redshifts, where the displacement due to the peculiar motion may be substantial. This will be particularly true if the sources in the sample being considered are

disproportionally larger in one of the two hemisphere, as it will cause a differential shift at different redshifts in the accordingly observed $m_B - z$ plot. Then adjusting a theoretical curve for a cosmological model to match with the observed $m_B - z$ plot at low redshifts ($z \lesssim 0.1$), might result, in turn, in a relative shift at high redshifts ($z \sim 1$).

More important, even the interpretation of the Hubble plot of SNe Ia and its comparisons with various cosmological models, suggesting an accelerating Hubble expansion [1–5, 8, 9] is based on the underlying assumption of the cosmological principle. Thus any doubts on the cosmological principle will lead to similar doubts in the conventional interpretation of the magnitude-redshift diagram of SNe Ia to estimate cosmological parameters and the inferences drawn in these as well as in most other important cosmological conclusions.

DATA AVAILABILITY

The data underlying this article are available in VizieR Astronomical Server in the public domain at <http://vizier.u-strasbg.fr/viz-bin/VizieR>. The dataset is downloadable by selecting catalog: J/A+A/568/A22/tablef3.

-
- [1] A. G. Riess et al. *Astron. J.* **116**, 1009-1038 (1998)
 - [2] S. Perlmutter et al. *Astrophys. J.* **517**, 565-586 (1999)
 - [3] M. Betoule et al. *Astr. Astrophys.*, **568**, A22 (2014)
 - [4] D. O. Jones et al. *Astrophys. J.* **857**, 51 (2018)
 - [5] D. M. Scolnic et al. *Astrophys. J.* **859**, 101 (2018)
 - [6] J. T. Nielsen, A. Guffanti, S. Sarkar, *Sci. Rep.* **6** 35596 (2016)
 - [7] J. Colin, R. Mohayaee, M. Rameez, and S. Sarkar, *Astr. Astrophys.*, **631**, L13 (2019)
 - [8] D. Rubin, B. Hayden, *Astrophys. J.* **833** L30 (2016)
 - [9] D. Rubin, J. Heitlauf, *Astrophys. J.* **894** 68 (2020)
 - [10] R. Mohayaee, M. Rameez, S. Sarkar, arXiv:2003.10420 (2020)
 - [11] D. Huterer, D. L. Shafer, F. Schmidt, *J. Cosm. Astropart. Phys.* **12** 33 (2015)
 - [12] A. Weyant, M. Wood-Vasey, L. Wasserman, P. Freeman, *Astrophys. J.* **732** 65 (2011)
 - [13] S. J. Turnbull, et al. *Mon. Not. R. Astron. Soc.* **420** 447 (2012)
 - [14] G. J. Mathews, et al. *Astrophys. J.* **827** 60 (2016)
 - [15] S. S. Boruah, M. J. Hudson, G. Lavaux, *Mon. Not. R. Astron. Soc.* **498** 2703 (2020)
 - [16] C. H. Lineweaver, et al., *Astrophys. J.*, **470**, 38-42 (1996).
 - [17] G. Hinshaw, et al., *Astrophys. J. Suppl. Ser.*, **180**, 225 (2009).
 - [18] N. Aghanim et al., *Astr. Astrophys.* **641**, A1 (2020)
 - [19] A. K. Singal *Astrophys. J.* **742**, L23-26 (2011)
 - [20] H. Rubart and D. J. Schwarz, *Astr. Astrophys.* **555**, A117 (2013)
 - [21] P. Tiwari, R. Kothari, A., Naskar, S., Nadkarni-Ghosh, and P. Jain *Astropart. Phys.*, **61**, 1-11 (2015)
 - [22] J. Colin, R. Mohayaee, M. Rameez and S. Sarkar *Mon. Not. Roy. Astron. Soc.*, **471** 1045-1055 (2017)
 - [23] C. A. P. Bengaly, R. Maartens and M. G. Santos *J. Cosm. Astropart. Phys.*, **4**, 31 (2018)
 - [24] A. K. Singal, *Phys. Rev. D*, **100**, 063501 (2019)
 - [25] A. K. Singal, *Mon. Not. Roy. Astron. Soc.*, **488**, L104 (2019)
 - [26] N. J. Secrest, S. V. Hausegger, M. Rameez, R. Mohayaee, S. Sarkar, and J. Colin, *Astrophys. J.* **908** L51 (2021)
 - [27] A. K. Singal, Proc. 1st Electronic Conference on Universe 2021 (ECU2021), doi:10.3390/ECU2021-09270 (2021)
 - [28] A. K. Singal, *Universe* **7** 107 (2021)
 - [29] T. M. Davis et al. *Astrophys. J.* **741**, 67 (2011)
 - [30] M. Rameez, arXiv:1905.00221 (2019)
 - [31] J. J. Condon et al. *Astr. J.* **115**, 1693-1716 (1998).
 - [32] N. J. Secrest, et al. *Astrophys. J. Suppl. Ser.* **221** 12 (2015)
 - [33] H. T. Intema, P. Jagannathan, K. P. Mooley and D. A. Frail *Astr. and Astrophys.*, **598**, A78, (2017)
 - [34] G. Swarup, S. Ananthkrishnan, V. K. Kapahi, A. P. Rao, C. R. Subrahmanya and V. K. Kulkarni *Current Science*, **60**, 95-105 (1991)
 - [35] I. Pàris et al., *Astr. Astrophys.*, **597**, A79 (2017)